Far East Journal of Applied Mathematics
Volume 58, Number 1, 2011, Pages 19-37
Published Online: November 2011
Available online at http://pphmj.com/journals/fjam.htm
Published by Pushpa Publishing House, Allahabad, INDIA

EFFECTS OF SLIP ON A TWO-LAYERED SUSPENSION MODEL FOR BLOOD FLOW THROUGH A CATHETERIZED ARTERY WITH A MILD OVERLAPPING STENOSIS

U. S. Chakraborty

Department of Mathematics
Assam University
Silchar-788011, India
e-mail: udayhkd@gmail.com

Abstract

The present study is concerned with the flow of blood in a catheterized artery with an overlapping mild stenosis. To account for the slip at stenotic wall, hematocrit and peripheral layer, blood has been represented by a two-layered macroscopic model consisting of a core region assumed to be a particle-fluid suspension and a peripheral layer of plasma (Newtonian fluid). The expression for the flow characteristics, namely, the axial velocities, the impedance, the wall shear stress, the shear stress at the critical height of the stenosis have been derived and represented graphically with respect to different flow parameters. The impedance increases with the hematocrit, stenosis size and radius of the catheter but decreases with slip at wall. It assumes lower magnitude in two-layered model than its corresponding value in one-layered model for any given hematocrit. With respect to any

2010 Mathematics Subject Classification: 76Z05.

Keywords and phrases: blood, hematocrit, slip, impedance, shear stress, peripheral plasma layer (PPL), catheter.

Received July 20, 2011

parameter, the shear stresses at the critical height possess the characteristics similar to that of impedance. Axial velocities increase with slip but decrease with radius of the catheter.

Introduction

Circulatory disorders are considered to be responsible for over seventy five percent of all deaths and atherosclerosis is one of the frequently occurring cardiovascular diseases [1]. The word atherosclerosis comes from the Greek words athero (meaning gruel or paste) and sclerosis (hardness) [2]. It is an abnormal and unnatural growth that develops at various locations of the cardiovascular system under diseased conditions and causes serious circulatory disorders. These disorders in circulatory systems include as, narrowing in body passage leading to the reduction and impediment to blood flow in the constricted artery regions, the blockage of the artery in making the flow irregular and causing an abnormality of the blood flow and, the presence of stenosis at one or more of the major blood vessels, carrying blood to the heart or brain etc., could lead to various arterial diseases e.g., myocardial infarction, angina pectoris, cerebral accident, coronary thrombosis, strokes, etc. [3, 4].

Blood being a suspension of corpuscles, behaves like a non-Newtonian fluid in small diameter tubes [5, 6]. The experimental observations of Cokelet [7] and theoretical investigation of Haynes [8] indicate that blood cannot be treated as a single-phase homogeneous viscous fluid while flowing through narrow arteries (of diameter $\leq 1000\,\mu\text{m}$). Skalak [9] concluded that an accurate description of the blood flow in small vessels requires the consideration of erythrocytes as discrete particles. Srivastava and Srivastava [10] concluded that blood can be suitably represented by a macroscopic two-phase model (i.e., a suspension of red cells in plasma) in small vessels (of diameter $\leq 2400\,\mu\text{m}$).

Bugliarello and Sevilla [11] and Cokelet [7] experimentally proved that for blood flowing through small vessels, there exist a cell-poor plasma (Newtonian fluid) layer and a core region of suspension of almost all the erythrocytes. Bugliarello and Sevilla [11] presented the flow of blood in small diameter tubes by a two-layered model assuming peripheral and core fluids as Newtonian fluids of different viscosities. Following the experimentally verified model of Bugliarello and Sevilla [11], two-fluid modeling of blood flow has been discussed and used by a good number of researchers. Shukla et al. [12] applied a two-fluid model to discuss the flow of blood through a stenosis. Shukla et al. [12], and Chaturani and Upadhya [13] addressed the flow of blood in small diameter tubes using the two-layered model of micropolar and couple stress fluids, respectively. Biswas and Chakraborty [15] analyzed the two layered model of blood flow in a stenosed artery considering blood as a Bingham plastic fluid in central core layer.

Cardiac catheterization (also called heart catheterization) is a diagnostic procedure that performs a comprehensive examination of functioning of the heart and its blood vessels [2]. In modern days, with the evolution of coronary balloon angioplasty, there has been a considerable increase in the use of catheters of various sizes. A catheter with a tiny balloon at the end is inserted into the artery in balloon angioplasty to treat atherosclerosis. The catheter is carefully guided to the location at which stenosis occurs and balloon is inflated to fracture the fatty deposits and widen the narrowed portion of the artery [16]. Back [17] and Back et al. [18] studied important hemodynamic characteristics like the wall shear stress, pressure drop, and frictional resistance in catheterized coronary arteries under normal as well as the pathological situation in presence of a stenosis. The effect of catheterization on various flow characteristics in a curved artery was studied by Karahalios [19] and Jayaraman and Tiwari [20]. Dash et al. [21] studied the changed flow pattern in a narrow artery when a catheter is inserted into it and estimated the increase in friction in the artery due to catheterization using a Casson fluid model for steady and pulsatile flow of blood. Sankar and Hemalatha [22] studied pulsatile flow of Herschel-Bulkley fluid through catheterized arteries. Srivastava and Rastogi [16] studied the steady flow of blood in a catheterized artery with a mild stenosis considering blood a particle-fluid suspension. Biswas and Chakraborty [23] analysed the effect of catheterization on pulsatile flow of blood in a stenosed artery.

In the most of the abovementioned studies, traditional no-slip boundary condition has been employed. However, a number of studies of suspensions in general and blood flow in particular both theoretical [24-28] and experimental [29, 30], have suggested the likely presence of slip (a velocity discontinuity) at the flow boundaries (or in their immediate neighbourhood). Recently, Ponalgusamy [31], Biswas and Chakraborty [23, 32, 33] have developed mathematical models for blood flow through stenosed arterial segment, by taking a velocity slip condition at the constricted wall. But to authors knowledge, no theoretical or experimental work has been done till date to analyze the effect of velocity slip at the stenotic wall on two-layered, macroscopic two-phase (plasma-red cell system) blood flow model in a catheterized artery.

With the above motivations, an attempt has been made to study the effects of slip (at the stenotic wall), peripheral plasma layer and hematocrit on the flow variables (wall shear stress, velocity profiles, and resistance to flow) for blood flow through a catheterized vessel with an overlapping mild stenosis taking into account that blood is represented by a particle-fluid suspension.

Mathematical Formulation

We consider an axially symmetric, laminar, steady and fully developed flow of blood (assumed to be incompressible) through a catheterized circular tube with an axially symmetric overlapping stenosis as shown in Figure 1.

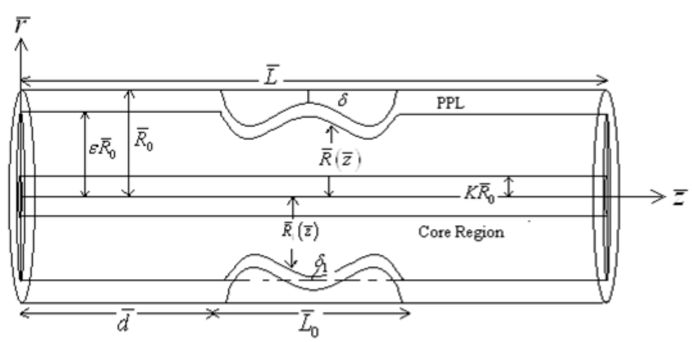

Figure 1. Geometry of a catheterized artery with an overlapping stenosis.

It is assumed that wall of the tube is rigid and the body fluid blood is represented by a two-fluid model with a core region of suspension of all erythrocytes and a peripheral layer of plasma (a Newtonian viscous fluid). The artery length is assumed to be large enough as compared to its radius so that the entrance, exit and special wall effects can be neglected.

The geometry of stenosis with the peripheral region is given by [1]

$$\bar{R}(\bar{z}) = \begin{cases} \bar{R}_0 - \dfrac{2\bar{\delta}}{\bar{L}_0^4}[11(\bar{z}-\bar{d})\bar{L}_0^3 - 47(\bar{z}-\bar{d})^2\bar{L}_0^2 & \bar{d} \le \bar{z} \le \bar{d} + \bar{L}_0, \\ \qquad + 72(\bar{z}-\bar{d})^3\bar{L}_0 - 36(\bar{z}-\bar{d})^4], & \\ \bar{R}_0, & \text{otherwise.} \end{cases} \tag{1}$$

The geometry of the stenosis in the core region is given by [1]

$$\bar{R}_1(\bar{z}) = \begin{cases} \varepsilon\bar{R}_0 - \dfrac{2\bar{\delta}_1}{\bar{L}_0^4}[11(\bar{z}-\bar{d})\bar{L}_0^3 - 47(\bar{z}-\bar{d})^2\bar{L}_0^2 & \bar{d} \le \bar{z} \le \bar{d} + \bar{L}_0, \\ \qquad + 72(\bar{z}-\bar{d})^3\bar{L}_0 - 36(\bar{z}-\bar{d})^4], & \\ \varepsilon\bar{R}_0, & \text{otherwise,} \end{cases} \tag{2}$$

where $\bar{R}(\bar{z})$ is the radius of the stenosed artery with peripheral layer; $\bar{R}_1(\bar{z})$ is the radius of the artery in the stenosed core region such that $\bar{R}_1(\bar{z}) = \varepsilon\bar{R}(\bar{z})$; ε is the ratio of the central core radius to the normal artery radius; $\bar{R}_0$, $\varepsilon\bar{R}_0$ are the radii of the normal artery and core region of the normal artery respectively; $\bar{\delta}$ is the height of the stenosis at a distance $\bar{z} = \bar{d} + \bar{L}_0/2$, called the critical height in the peripheral region; $\bar{\delta}_1$ is the critical height of the stenosis in the core region such that $\bar{\delta}_1 = \varepsilon\bar{\delta}$, $\bar{L}_0$ is the length and $\bar{d}$ is the location of the stenosis. The appropriate equations governing the steady flow of a particle-fluid suspension in the case of a mild stenosis $(\bar{\delta}/\bar{R} \ll 1)$, subject to the additional conditions [2, 3, 10], $\mathrm{Re}(2\bar{\delta}/\bar{L}_0) \ll 1$, $2\bar{R}_0/\bar{L}_0 \sim O(1)$, can be written as

$$\frac{d\bar{p}}{d\bar{z}} = \frac{\bar{\mu}_0}{\bar{r}}\frac{\partial}{\partial\bar{r}}\left(\bar{r}\frac{\partial\bar{u}_0}{\partial\bar{r}}\right), \ \bar{R}_1 \le \bar{r} \le \bar{R}, \tag{3}$$

$$(1-C)\frac{d\bar{p}}{d\bar{z}} = (1-C)\frac{\bar{\mu}_s(C)}{\bar{r}}\frac{\partial}{\partial\bar{r}}\left(\bar{r}\frac{\partial\bar{u}_f}{\partial\bar{r}}\right) + C\bar{S}(\bar{u}_p - \bar{u}_f), \ k\bar{R}_0 \le \bar{r} \le \bar{R}_1, \tag{4}$$

$$C\frac{d\bar{p}}{d\bar{z}} = CS(\bar{u}_f - \bar{u}_p), \quad k\bar{R}_0 \le \bar{r} \le \bar{R}_1, \tag{5}$$

where $(\bar{r}, \bar{z})$ are (radial, axial) coordinates, $(\bar{u}_p, \bar{u}_f)$ are the axial velocities of (particle, fluid) in the core region $(0 \le \bar{r} \le \bar{R}_1)$, $(\bar{\mu}_0, \bar{u}_0)$ are the (viscosity, fluid velocity) in the peripheral region $(\bar{R}_1 \le \bar{r} \le \bar{R})$, $\bar{\mu}_s \cong \bar{\mu}_s(C)$ is the suspension viscosity in the core region, C denotes the constant volume fraction density of the particles (called hematocrit) and $\bar{S}$ is the drag coefficient of interaction between the two phases (fluid and particle). The expression for the drag coefficient of interaction $\bar{S}$ and empirical relation for the viscosity of suspension $\bar{\mu}_s$ may be selected [1, 2, 16] as

$$\bar{S} = \frac{9}{2}\frac{\bar{\mu}_0}{\bar{a}_0^2}\frac{[4 + 3(8C - 3C^2)^{1/2} + 3C]}{(2-3C)^2}, \tag{6}$$

$$\bar{\mu}_s = \frac{\bar{\mu}_0}{1 - qC}; \ q = 0.07\exp\left[2.49C + \frac{1107^\circ K}{T}\exp(-1.69C)\right], \tag{7}$$

where $\bar{a}_0$ is the radius of a particle and T is measured in absolute temperature.

Boundary conditions associated with the problem are given by

$$\bar{u}_0 = \bar{u}_s \ \text{at} \ \bar{r} = \bar{R}, \tag{8}$$

$$\bar{u}_0 = \bar{u}_f, \ \bar{\tau}_0 = \bar{\tau}_f \ \text{at} \ \bar{r} = \bar{R}_1, \tag{9}$$

$$\bar{u}_f = 0 \ \text{at} \ \bar{r} = k\bar{R}_0, \tag{10}$$

where $\bar{u}_s$ is the axial velocity slip at the stenotic wall [15, 23, 32, 33], $k\bar{R}_0 (k \ll 1)$ is the radius of the axisymmetric catheter and $\bar{\tau}_0 = \bar{\mu}_0 \dfrac{\partial \bar{u}_0}{\partial \bar{r}}$, $\bar{\tau}_f = (1 - C)\bar{\mu}_s \dfrac{\partial \bar{u}_f}{\partial \bar{r}}$ are the shear stresses in the peripheral and central core region, respectively.

We introduce the following non-dimensional variables:

$$z = \bar{z}/\bar{R}_0,\ d = \bar{d}/\bar{R}_0,\ (R,\ R_1,\ k) = (\bar{R},\ \bar{R}_1,\ k\bar{R}_0)/\bar{R}_0,$$

$$(\delta,\ \delta_1) = (\bar{\delta},\ \bar{\delta}_1)/\bar{R}_0,\ \mu_s = \bar{\mu}_s/\bar{\mu}_0,\ \bar{S} = \frac{S}{\bar{\mu}_0/\bar{R}_0},$$

$$\frac{d\bar{p}}{d\bar{z}} = \frac{dp}{dz}/\bar{q}_0,\ (u_0,\ u_f,\ u_p) = \frac{(\bar{u}_0,\ \bar{u}_f,\ \bar{u}_p)}{\bar{q}_0\bar{R}_0^2/4\bar{\mu}_0},$$

$$(\tau_0,\ \tau_f) = \frac{(\bar{\tau}_0,\ \bar{\tau}_f)}{\bar{q}_0\bar{R}_0/2},\ (L,\ L_0) = \frac{(\bar{L},\ \bar{L}_0)}{\bar{R}_0}, \tag{11}$$

where $\bar{q}_0$ is the negative of the pressure gradient in a uniform tube without stenosis and $\bar{L}$ is the length of the stenosed artery.

The non-dimensional form of the geometry of stenosis with the help of equation (11) can be given by

$$(R,\ R_1) = \begin{cases} (1,\ \varepsilon) - \dfrac{2(\delta,\ \delta_1)}{L_0^4}[11(z-d)L_0^3 - 47(z-d)^2 L_0^2 & d \le z \le d + L_0, \\ \qquad\qquad + 72(z-d)^3 L_0 - 36(z-d)^4], & \\ (1,\ \varepsilon), & \text{otherwise.} \end{cases} \tag{12}$$

Using the non-dimensional variables given in (11), equations (3)-(5) become

$$\frac{dp}{dz} = \frac{1}{r}\frac{\partial}{\partial r}\left(r\frac{\partial u_0}{\partial r}\right),\ R_1 \le r \le R, \tag{13}$$

$$(1-C)\frac{dp}{dz} = (1-C)\frac{\mu_s}{r}\frac{\partial}{\partial r}\left(r\frac{\partial u_f}{\partial r}\right) + CS(u_p - u_f),\ k \le r \le R_1, \tag{14}$$

$$C\frac{dp}{dz} = CS(u_f - u_p),\ k \le r \le R_1. \tag{15}$$

The boundary conditions in non-dimensional form are given by

$$u_0 = u_s \ \text{at}\ r = R, \tag{16}$$

$$u_0 = u_f,\ \tau_0 = \tau_f \ \text{at}\ r = R_1, \tag{17}$$

$$u_f = 0 \ \text{at}\ r = k. \tag{18}$$

The non-dimensional volumetric flow rate is given by

$$Q = \frac{\overline{Q}}{\pi(\overline{R}_0)^4\overline{q}_0/8\overline{\mu}_0} = 4\left\{\int_k^{R_1}[(1-C)u_f + Cu_p]dr + \int_{R_1}^{R} ru_0 dr\right\}, \tag{19}$$

where $\overline{Q} = 2\pi\left\{\int_{k\overline{R}_0}^{\overline{R}_1}\overline{r}[(1-C)\overline{u}_f + C\overline{u}_p]d\overline{r} + \int_{\overline{R}_1}^{\overline{R}}\overline{r}\,\overline{u}_0 d\overline{r}\right\}$ is the volumetric flow rate.

The non-dimensional shear stresses are given by

$$\tau_0 = \frac{1}{2}\frac{\partial u_0}{\partial r},\ \tau_f = \frac{(1-C)\mu_s}{2}\frac{\partial u_f}{\partial r}, \tag{20}$$

Solution

Solving equations (13)-(15) with the help of boundary conditions (16)-(18), we get

$$u_0 = \left\{1 - \frac{(1-C)\mu_s\log(r/R)}{\alpha+\beta}\right\}u_s$$

$$-\frac{dp}{dz}\left\{(R^2 - r^2) - \frac{(1-C)\mu_s(R^2 - R_1^2) + (R_1^2 - k^2)}{\alpha+\beta}\log(r/R)\right\},$$

$$R_1 \le r \le R, \tag{21}$$

$$u_f = \left\{1 - \frac{\alpha + \log(r/R_1)}{\alpha + \beta}\right\} u_s$$

$$- \frac{dp}{dz}\left\{(R^2 - R_1^2) + \frac{R_1^2 - r^2}{(1-C)\mu_s} - \frac{\left\{(R^2 - R_1^2) + \frac{(R_1^2 - k^2)}{(1-C)\mu_s}\right\}}{\alpha + \beta}\{\alpha + \log(r/R_1)\}\right\},$$

$$k \le r \le R_1, \tag{22}$$

$$u_p = \left\{1 - \frac{\alpha + \log(r/R_1)}{\alpha + \beta}\right\} u_s$$

$$- \frac{dp}{dz}\left\{(R^2 - R_1^2) + \frac{R_1^2 - r^2}{(1-C)\mu_s} - \frac{\left\{(R^2 - R_1^2) + \frac{(R_1^2 - k^2)}{(1-C)\mu_s}\right\}}{\alpha + \beta}\{\alpha + \log(r/R_1)\} + \frac{4C}{S}\right\},$$

$$k \le r \le R_1, \tag{23}$$

where

$$\alpha = (1-C)\mu_s \log(\varepsilon) \ \text{ and } \ \beta = \log(k/R_1).$$

From equation (19), the non-dimensional flow rate is given by

$$Q = \left[\left\{\frac{1-(1-C)\mu_s}{\alpha+\beta}\right\}R_1^2 + \left\{2 + \frac{(1-C)\mu_s}{\alpha+\beta}\right\}R^2 - \left(\frac{1}{\alpha+\beta}\right)k^2\right]u_s$$

$$- \frac{dp}{dz}\left[(R^2 - R_1^2)(R^2 + R_1^2 - k^2) + \frac{(R_1^2 - k^2)^2}{(1-C)\mu_s} + \left\{(R^2 - R_1^2) + \frac{(R_1^2 - k^2)}{(1-C)\mu_s}\right\}\right.$$

$$\left. \times \left\{\frac{(1-(1-C)\mu_s)}{\alpha+\beta}R_1^2 + \frac{(1-C)\mu_s}{\alpha+\beta}R^2 + \left(2 - \frac{1}{\alpha+\beta}\right)k^2\right\} + \frac{8C}{S}(R_1^2 - k^2)\right]. \tag{24}$$

The pressure gradient $\frac{dp}{dz}$ can easily be obtained out by taking $Q = 1$ [4] as

$$\frac{dp}{dz} = \left(\left[\left\{\frac{1-(1-C)\mu_s}{\alpha+\beta}\right\}R_1^2 + \left\{2+\frac{(1-C)\mu_s}{\alpha+\beta}\right\}R^2 - \left(\frac{1}{\alpha+\beta}\right)k^2\right]u_s - 1\right)$$
$$\times\left[(R^2-R_1^2)(R^2+R_1^2-k^2)+\frac{(R_1^2-k^2)^2}{(1-C)\mu_s}+\left\{(R^2-R_1^2)+\frac{(R_1^2-k^2)}{(1-C)\mu_s}\right\}\right.$$
$$\left.\times\left\{\frac{(1-(1-C)\mu_s)}{\alpha+\beta}R_1^2+\frac{(1-C)\mu_s}{\alpha+\beta}R^2+\left(2-\frac{1}{\alpha+\beta}\right)k^2\right\}+\frac{8C}{S}(R_1^2-k^2)\right]^{-1}. \tag{25}$$

The resistance to flow (impedance) is given by

$$\lambda = \frac{\Delta p}{Q} = \int_0^L\left(-\frac{dp}{dz}\right)dz$$
$$= \int_0^d\left(-\frac{dp}{dz}\right)_{R=1}dz + \int_d^{d+L_0}\left(-\frac{dp}{dz}\right)dz + \int_{d+L_0}^{L}\left(-\frac{dp}{dz}\right)_{R=1}dz. \tag{26}$$

The first and the third integrals in the expression for λ (equation (24)) are straight forward where as the analytical evaluation of the second integral is a formidable task. In view of this, one obtains the final expression for the flow resistance, λ as

$$\lambda = G(L-L_0) + \int_d^{d+L_0}\left(-\frac{dp}{dz}\right)dz. \tag{27}$$

In equation (25), expression for G is given by

$$G = \left(1-\left[\left\{\frac{1-(1-C)\mu_s}{\alpha+\gamma}\right\}\varepsilon^2 + \left\{2+\frac{(1-C)\mu_s}{\alpha+\gamma}\right\} - \left(\frac{1}{\alpha+\gamma}\right)k^2\right]u_s\right)$$
$$\times\left[(1-\varepsilon^2)(1+\varepsilon^2-k^2)+\frac{(\varepsilon^2-k^2)^2}{(1-C)\mu_s}+\left\{(1-\varepsilon^2)+\frac{(\varepsilon^2-k^2)}{(1-C)\mu_s}\right\}\right.$$
$$\left.\times\left\{\frac{(1-(1-C)\mu_s)}{\alpha+\gamma}\varepsilon^2+\frac{(1-C)\mu_s}{\alpha+\gamma}+\left(2-\frac{1}{\alpha+\gamma}\right)k^2\right\}+\frac{8C}{S}(\varepsilon^2-k^2)\right]^{-1}, \tag{28}$$

where $\gamma = \log\left(\frac{K}{\varepsilon}\right)$.

The expression for the wall shear stress can be obtained from equation (20) as

$$\tau_R = \left(\frac{1}{2}\frac{\partial u_0}{\partial r}\right)_{r=R}$$

$$= -\frac{(1-C)\mu_s}{2(\alpha+\beta)}u_s + \frac{dp}{dz}\left\{R + \frac{(1-C)\mu_s(R^2 - R_1^2) + (R_1^2 - k^2)}{2R(\alpha+\beta)}\right\}. \quad (29)$$

The shear stress at the critical height of the stenosis is given by

$$\tau_S = \left(\frac{1}{2}\frac{\partial u_0}{\partial r}\right)_{r=(1-\delta)} = -\frac{(1-C)\mu_s}{2(\alpha+\beta)}u_s$$

$$+ \frac{dp}{dz}\left[(1-\delta) + \frac{(1-C)\mu_s(1-\varepsilon^2)(1-\delta)^2 + \{\varepsilon^2(1-\delta)^2 - k^2\}}{2(1-\delta)\{\alpha + \log(k/\varepsilon(1-\delta))\}}\right]. \quad (30)$$

In absence of catheter $(k \to 0)$ and slip at wall $(u_s = 0)$, the present study reduces to the analysis performed by Srivastava et al. [1].

Results and Discussions

To analyze the quantitative effects of volume fraction density of the particles (hematocrit) C, the critical height attained by the overlapping stenosis δ, the radius of the catheter k, the ratio of the central core radius to the normal artery radius ε, slip velocity at stenotic wall u_s, computer codes have been developed for numerical evaluations of the analytic results obtained for u_0, u_f, λ, τ_R and τ_S in equations (21), (22), (27), (29), (30) for parameter values $C = 0 - 0.6$; $\delta = 0 - 0.2$; $\varepsilon = 0.8 - 1$; $k = 0, 0.1, 0.2$; $u_s = 0, 0.02, 0.05$; $a_0 = 4\,\mu\text{m}$; $T = 37^\circ\text{C}$ [1]. The variation of resistance to flow λ with critical height of the stenosis δ for different values of parameters k and u_s is presented in Figure 2. The variation of λ with hematocrit parameter C for different values of k, u_s and the variation of λ with ε for different values of k, C have been depicted in Figures 3 and 4, respectively. Also, the variations of τ_S with δ is depicted in Figure 5, with C in Figure 6 for different values of the parameters k, u_s and with ε in Figure 7 for different values of *k*, *C*. Figure 8 shows the variation of the wall shear stress distribution with axial distance *z* for different values of *k* and *C*. Finally, the variations of u_0 and u_f with radial distance *r* for different values of *k* and u_s are displayed in Figure 9.

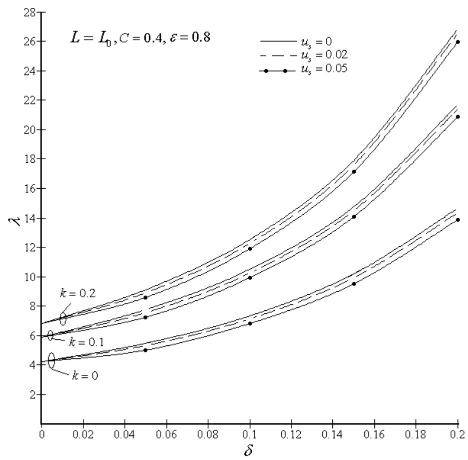

Figure 2. Variation of resistance to flow λ with critical height of the stenosis δ for different values of *k* and u_s.

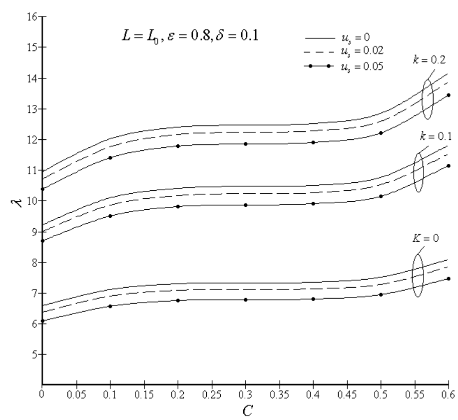

Figure 3. Variation of resistance to flow λ with hematocrit parameter *C* for different values of *k* and u_s.

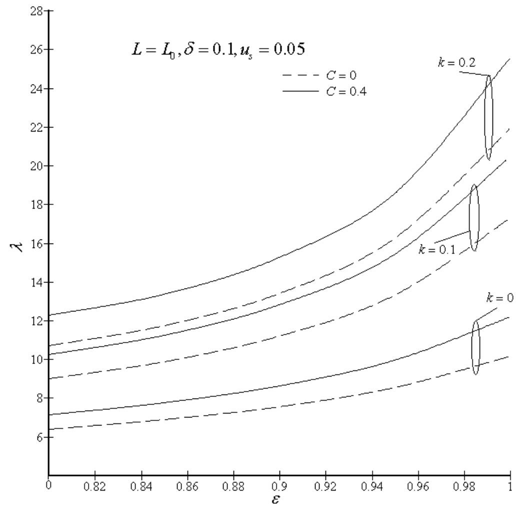

Figure 4. Variation of resistance to flow λ with ε for different values of *k* and *C*.

In Figures 2-4, it is clearly noticed that the resistance to flow λ, experienced by the streaming fluid over the whole arterial segment increases with the hematocrit *C*, the critical height of the stenosis δ, radius of the inserted catheter *k* and the ratio ε but decreases with the slip velocity attained by the fluid at the constricted wall. For any value of the catheter radius *k* as the hematocrit *C* increases from 0 to 0.1, resistance to flow λ increases steeply, the increment is relatively slower from $C = 0.1$ to 0.5 and then again it starts increasing rapidly from $C = 0.5$ to 0.6. However, employment of velocity slip at wall decreases the resistance for any value of *k* and *C*.

It is observed from Figures 5-7 that the wall shear stress at the critical height of the stenosis τ_S increases with δ and *C* for any values of catheter radius *k* but decreases with velocity slip u_S at the stenotic wall. As the ratio of the central core radius to the normal artery radius ε increases, τ_S increases gradually and the maximum magnitude is attained at $\varepsilon = 1$, i.e., for single layered flow. Also, for any value of ε (i.e., for both single and two-layered flow), increase in catheter radius *k* increases τ_S.

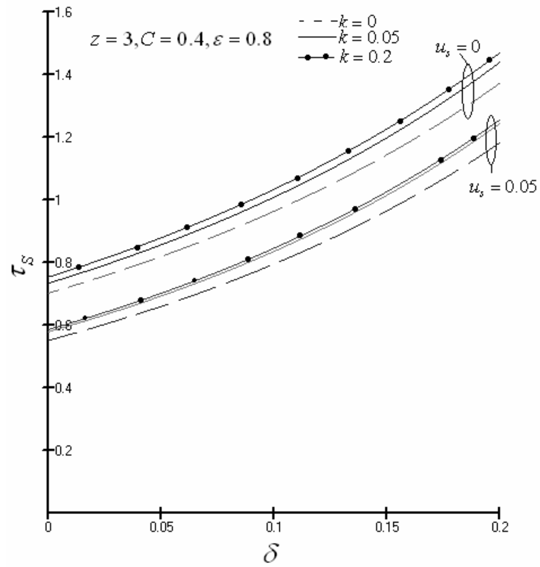

Figure 5. Variation of shear stress at the critical height τ_S with δ for different values of k and u_s.

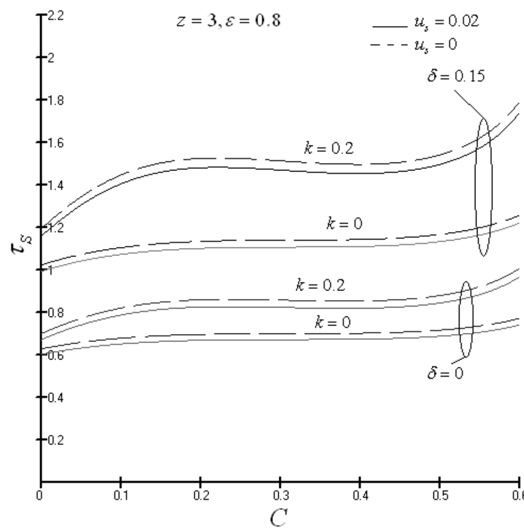

Figure 6. Variation of shear stress at the critical height τ_S with C for different values of k and u_s.

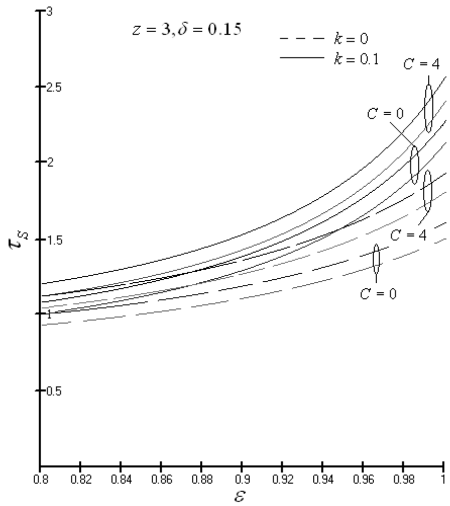

Figure 7. Variation of shear stress at the critical height τ_S with ε for different values of *k* and *C*.

From Figure 8, it is revealed that the wall shear stress in the stenotic region, τ_R rapidly increases from its approached value at $z = 0$ to its peak value in the upstream of the first stenosis throat at $z = 3 - \sqrt{7/2} \simeq 1,$ it then decreases steeply in the downstream of the first throat to its magnitude at the critical height of the stenosis at $z = 3.$ The flow characteristic, τ_R further increases steeply in the upstream of the second stenosis throat and attains its peak magnitude (same as at the first throat of the stenosis) at the second throat of the stenosis at $z = 3 + \sqrt{7/2} \simeq 5,$ it then decreases rapidly to the same magnitude as its approached value (at $z = 0$) at the end point of the constriction profile at $z = 6.$ It is also observed that the wall shear stress τ_R at any axial distance increases with catheter radius *k* and hematocrit *C*.

Figure 9 shows that the axial velocity in the core region u_f increases with radial distance *r* until it reaches its maximum wherefrom it starts decreasing and equals with axial velocity in peripheral region u_0 at $r = \varepsilon$ an comes to its minimum at the stenotic wall $(r = R).$ It is noticed that axial velocities both in core and peripheral regions increases with velocity slip u_s but decreases with catheter radius *k*.

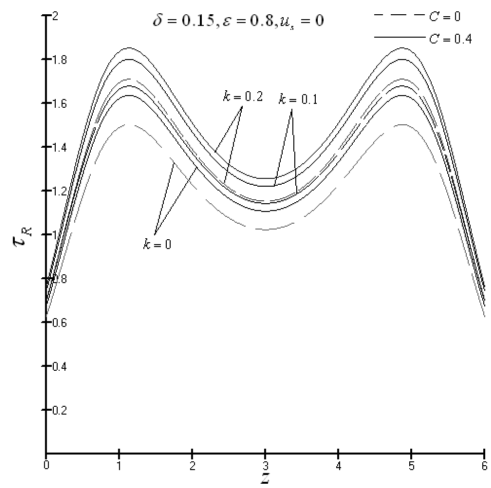

Figure 8. Variation of wall shear stress τ_R with axial distance *z* for different values of *k* and *C*.

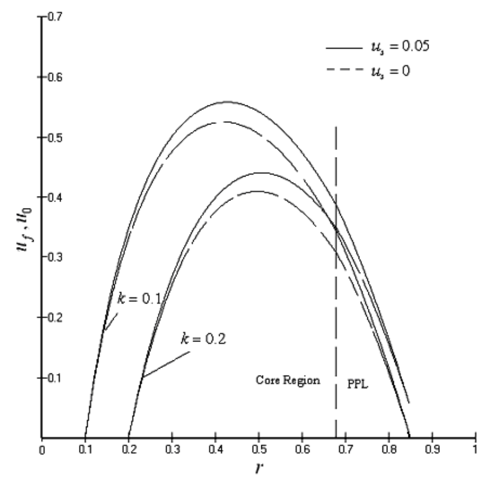

Figure 9. Variation of axial velocities u_f and u_0 with radial distance *r* for different values of *k* and u_s.

Conclusion

To observe the effects of slip velocity, hematocrit and the peripheral layer on flow characteristics of blood, a two-layered model, assuming that blood in the central region is represented by a suspension of erythrocytes in plasma, has been applied to discuss the flow through an overlapping stenosis in a catheterized artery. The flow characteristics (resistance to flow, wall shear stress in the stenotic region, and shear stress at the critical height of the stenosis) increase with hematocrit, catheter radius and also with stenosis height. These flow variables assume lower magnitude in two-layered model than its corresponding value in one-layered model. Again employment of velocity slip at stenotic wall reduces their magnitude. These conclude that the presence of velocity slip and peripheral layer helps in the normal functioning of the diseased artery. The shear stress at the two stenosis throats assumes the same magnitude. The axial velocities both in central core and peripheral regions increase with velocity slip.

Throughout a number of restrictions have been imposed on the present study and lots of simplifications have been made, but still it enables someone to estimate the effects of slip velocity at the stenotic wall, hematocrit and peripheral layer on flow characteristics of blood flowing through a catheterized artery with an overlapping mild constriction. The model would have been more realistic if pulsatile flow and permeability of the arterial wall were considered. Also the consideration of non-uniform artery could have brought the analysis nearer to actual situation. Those are the scopes for future course of study.

References

[1] V. P. Srivastava, R. Rastogi and R. Vishnoi, A two-layered suspension blood flow through an overlapping stenosis, Comput. Math. Appl. 60 (2010), 432-441.

[2] K. S. Mekheimer and M. A. E. Kot, Suspension model for blood flow through arterial catheterization, Chem. Eng. Comm. 197 (2010), 1195-1214.

[3] D. F. Young, Effects of a time-dependent stenosis of flow through a tube, J. Eng. Ind. 90 (1968), 248-254.

[4] D. S. Sankar and U. Lee, Mathematical modeling of pulsatile flow of non-Newtonian fluid in stenosed arteries, Commun. Nonlinear. Sci. Numer. Simulat. 14 (2009), 2971-2981.

[5] F. W. Merrill, A. M. Benis, E. R. Gilliland, T. K. Sherwood and E. W. Salzman, Pressure-flow relations of human blood in hallow fibers at low flow rates, J. Appl. Physiol. 20 (1965), 954-967.

[6] S. E. Charm and G. S. Kurland, Blood Flow and Micro Circulation, John Wiley, New York, 1974.

[7] G. R. Cokelet, The Rheology of Human Blood, Y. C. Fung et al. eds., Biomechanics: Its foundation and objectives, Englewood Cliffs, NJ, Prentice-Hall, 1972.

[8] R. H. Haynes, Physical basis on dependence of blood viscosity on tube radius, Am. J. Physiol. 198 (1960), 1193-1205.

[9] R. Skalak, Mechanics of Microcirculation: Biomechanics, its Foundation and Objectives, Y. C. Fung, ed., Prentice Hall Publ. Co., Englewood Cliffs, 1972.

[10] L. M. Srivastava and V. P. Srivastava, On two-phase model of pulsatile blood flow with entrance effects, Biorheol. 20 (1983), 761-777.

[11] G. Bugliarello and J. Sevilla, Velocity distribution and other characteristics of steady and pulsatile blood flow in fine glass tubes, Biorheol. 7 (1970), 85-107.

[12] J. B. Shukla, R. S. Parihar and S. P. Gupta, Effects of peripheral layer viscosity on blood flow through an artery with mild stenosis, Bull. Math. Biol. 42 (1980), 797-805.

[13] P. Chaturani and V. S. Upadhya, On micropolar fluid model for blood flow through narrow tubes, Biorheol. 16 (1979), 419-428.

[14] P. Chaturani and V. S. Upadhya, A two-fluid model for blood flow through small diameter tubes with non-zero couple stress boundary condition at the interface, Biorheol. 18 (1981), 245-253.

[15] D. Biswas and U. S. Chakraborty, Two-layered pulsatile blood flow in a stenosed artery with body acceleration and slip at wall, Appl. Appl. Math. 5(10) (2010), 1400-1417.

[16] V. P. Srivastava and R. Rastogi, Blood flow through stenosed catheterized artery: effects of hematocrit and stenosis shape, Comput. Math. Appl. 59 (2010), 1377-1385.

[17] L. H. Back, Estimated mean flow resistance increase during coronary artery catheterization, J. Biomech. 27 (1994), 169-175.

[18] L. H. Back, E. Y. Kwack and M. R. Back, Flow rate-pressure drop relation in coronary angioplasty: Catheter obstruction effect, J. Biomech. Eng. 118 (1996), 83-89.

[19] G. T. Karahalios, Some possible effects of a catheter on the arterial wall, Med. Phys. 17 (1990), 922-925.

[20] G. Jayaraman and K. Tiwari, Flow in a catheterized curved artery, Med. Biol. Eng. Comput. 33 (1995), 1-6.

[21] R. K. Dash, G. Jayaraman and K. N. Mehta, Estimation of increased flow resistance in a narrow catheterized artery-A theoretical model, J. Biomech. 29 (1996), 917-930.

[22] D. S. Sankar and K. Hemalatha, Pulsatile flow of Herschel-Bulkley fluid through catheterized arteries-A mathematical model, Appl. Math. Model. 31 (2007), 1497-1517.

[23] D. Biswas and U. S. Chakraborty, Pulsatile blood flow through a catheterized artery with an axially non-symmetrical stenosis, Appl. Math. Sci. 4 (2010), 2865-2880.

[24] V. Vand, Viscosity of solutions and suspensions, J. Phys. Colloid. Chem. 52 (1948), 277-321.

[25] A. L. Jones, On the flow of blood in a tube, Biorheol. 3 (1966), 183-188.

[26] P. Brunn, The velocity slip of polar fluids, Rheol. Acta. 14 (1975), 1039-1054.

[27] Y. Nubar, Effects of slip on the rheology of a composite fluid: application to blood flow, Rheol. 4 (1967), 133-150.

[28] P. Chaturani and D. Biswas, A comparative study of Poiseuille flow of a polar fluid under various boundary conditions with applications to blood flow, Rheol. Acta. 23 (1984), 435-445.

[29] G. Bugliarello and J. W. Hayden, High speed micro cinematographic studies of blood flow in vitro, Science 138 (1962), 981-983.

[30] L. Bennet, Red cell slip at a wall in vitro, Science 155 (1967), 1554-1556.

[31] R. Ponalgusamy, Blood flow through an artery with mild stenosis: a two-layered model, different shapes of stenoses and slip velocity at the wall, J. Appl. Sci. 7 (2007), 1071-1077.

[32] D. Biswas and U. S. Chakraborty, Pulsatile flow of blood in a constricted artery with body acceleration, Appl. Math. 4 (2009), 329-342.

[33] D. Biswas and U. S. Chakraborty, Pulsatile flow of blood in a constricted artery with a velocity slip, Far East J. Appl. Math. 36(3) (2009), 331-342.